Advances in Materials Physics and Chemistry, **2011, 1, 7-13**
doi:10.4236/ampc.2011.12002 Published Online September 2011 (http://www.SciRP.org/journal/ampc)

Synthesis, Structure and Magnetic Properties of CoNi Submicrospherical Chains*

Yajing Zhang[1], Siu-Wing Or[1], Zhidong Zhang[2]
[1]*Department of Electrical Engineering, Hong Kong Polytechnic University, Hung Hom, Hong Kong, China*
[2]*Shenyang National Laboratory for Materials Science, Institute of Metal Research and International Centre for Materials Physics, Chinese Academy of Sciences, Shenyang, China*
E-mail: *eeswor@polyu.edu.hk*
Received July 1,2011; *revised August* 14, 2011; *accepted August* 25, 2011

Abstract

High-purity magnetic CoNi submicrospherical chains, each of length 20 μm - 30 μm and self-assembled from fcc-phase CoNi submicrospheres of average diameter 800 nm, are synthesized via a surfactant-assisted solvothermal route without the aid of nucleation agent. The effects of surfactant and reducing agent on the morphology and size of the CoNi chains are studied, and a possible growth mechanism for the CoNi chains is proposed. The CoNi chains show ferromagnetic characteristics with a similarly small saturation magnetization of 104.1 emu/g and a larger coercivity of 150 Oe at room temperature compared to the monodispersed CoNi submicrospheres of 105 emu/g and 34 Oe as a result of the increased shape anisotropy.

Keywords: Chain-Like Assembles, CoNi, Magnetic Properties, Morphology, Solvothermal Route, Submicrospherical Chains

1. Introduction

Magnetic nanomaterials have received much attention in recent years because of their unique magnetic properties and high application potential for data storages, microelectronic devices, medical diagnosis, catalysis, etc. [1,2]. In fact, the magnetic properties of magnetic nanomaterials depend greatly on their size and shape [3]. Most of the isolated magnetic nanoparticles with sizes below a critical value (e.g. diameter < 10 nm for CoNi particles) are superparamagnetic at room temperature and thus are inappropriate for many fields of applications [4]. In view of this, there is an increasing driving force pushing towards the synthesis of magnetic nanomaterials with various nanostructures in order to increase the shape anisotropy for possible ferromagnetism [5-7].

Among various magnetic metals, CoNi is regarded as an important magnetic alloy due to its attractive magnetic and catalytic properties as well as improved mechanical properties compared to Co [8]. In the past decade, a variety of methods have been developed to synthesize micro- and nanosized CoNi particles such as sol-gel routes, electrodeposition, sonochemical synthesis, decomposition of organometallic precursors, polyol reduction and hydrothermal routes [9-15]. Recently, several CoNi assemblies have also been synthesized, including sea-urchin-like particles prepared using CoNi nanowires as building block by heterogeneous nucleation in liquid polyol [16], chain-like CoNi assemblies synthesized by a surfactant-assisted hydrothermal route [17] and single-walled flux-closure CoNi magnetic nanorings synthesized using triethylene glycol as solvent in the presence of poly (vinylpyrrolidone) [18]. With the preliminary remarks on CoNi assemblies, continual research effort is required to explore other possible synthesis methods, interesting assemblies, the relationship between structure and properties, etc.

In this work, we present the synthesis and structure of highly anisotropic, highly pure CoNi submicrospherical chains self-assembled from fcc-phase CoNi submicrospheres via a surfactant-assisted solvothermal route without involving any nucleation agent. The influence of both surfactant and reducing agent on the morphology and size of the submicrospheres is discussed, together with a possible growth mechanism for the CoNi chains. The magnetic properties of the CoNi chains are also investi-

*This work was supported by the Research Grants Council of the HKSAR Government (PolyU 5266/08E), The Hong Kong Polytechnic University (1-ZV7P, 4-ZZ7L and G-U741), and the National Nature Science Foundation of China (50331030).

Copyright © 2011 SciRes.

gated by measuring their magnetic hysteresis loops as well as zero field-cooled and field-cooled magnetizations at various temperatures.

2. Experimental Details

In the proposed surfactant-assisted solvothermal route, cobalt (II) chloride hexahydrate ($CoCl_2 \cdot 6H_2O$) and nickel (II) chloride hexahydrate ($NiCl_2 \cdot 6H_2O$) were used as precursors, while poly (vinyl pyrrolidone) (PVP), hydrazine monohydrate ($N_2H_4 \cdot H_2O$) and ethylene glycol (EG) were employed as surfactant, reducing agent and base solution, respectively. These reagents were commercial acquired with analytical pure and without further purification. In a typical synthesis procedure, 0.5 mmol (0.12 g) of $CoCl_2 \cdot 6H_2O$, 0.5 mmol (0.12 g) of $NiCl_2 \cdot 6H_2O$ and 2.1 mmol (0.5 g) of PVP were dissolved in 30 mL of EG, and the solution was stirred steadily for 30 min at room temperature. After adding 2 mL of $N_2H_4 \cdot H_2O$, the solution was further stirred for 30 min. The stirred solution was transferred into a Teflon-lined stainless steel autoclave of volume 50 ml. The autoclave was subsequently sealed and maintained at 200˚C for 2 h before being cooled to room temperature naturally. The as-prepared product was filtered off, washed with distilled water and ethanol for several times, and dried in a vacuum oven at 60˚C for 4 h. Control experiments were carried out by adjusting the amounts of PVP (from 0 g to 1 g) and $N_2H_4 \cdot H_2O$ (from 0 mL to 3 mL), while keeping other reaction parameters unchanged.

The phase and purity of all the as-prepared products were identified by a Rigaku D/max 2500pc X-ray diffractometer with Cu-$K\alpha$ radiation (λ = 1.54156 Å) at a scan rate of 0.04˚/s. The morphology and size were characterized by a JEOL JSM-6335F field emission scanning electron microscope equipped with an energy-dispersive X-ray spectrometer and operated at an emission voltage of 15 kV. The detailed morphology was investigated using a JEOL2010 transmission electron microscope with an emission voltage of 200 kV. The magnetic hysteresis loops were measured at both 5 K and 295 K (room temperature) using a MPMS-7 superconducting quantum interference device (SQUID) magnetometer for magnetic fields up to 20 kOe. The temperature dependence of zero field-cooled and field-cooled magnetizations was also measured using the SQUID magnetometer in the temperature range of 5 K - 295 K.

3. Results and Discussion

3.1. Structure, Morphology and Size

Figure 1 shows a typical X-ray diffraction (XRD) pattern of the product synthesized at 200˚C for 2 h. Three sharp XRD peaks are observed at 44.34˚, 51.65˚ and 76.14˚, corresponding to the (111), (200) and (220) planes, respectively. The appearance of these peaks in the XRD pattern indicates the existence of a face centered cubic (fcc) phase in the product. Apart from these peaks, the XRD pattern is essentially clean with no other detectable peaks, especially for those caused by impurities such as $Co(OH)_2$ or $Ni(OH)_2$. This suggests that the reduction reaction in our solvothermal route is rather complete.

Figure 2 plots a typical energy-dispersive X-ray spectroscopy (EDS) spectrum of the product synthesized at 200˚C for 2 h. Four different types of elements are detected, including Co, Ni, Au and Si. The presence of Au element in the EDS spectrum originates from the sputtered thin Au layer on the product for the test purpose, while the occurrence of Si element results from the use of a silicon wafer to support the product. Excluding these two types of elements, the mean molar ratio of Co to Ni in the product at different selected locations is approximately 0.96 (49:51). This value not only agrees with the starting stoichiometric proportion, but also confirms, in

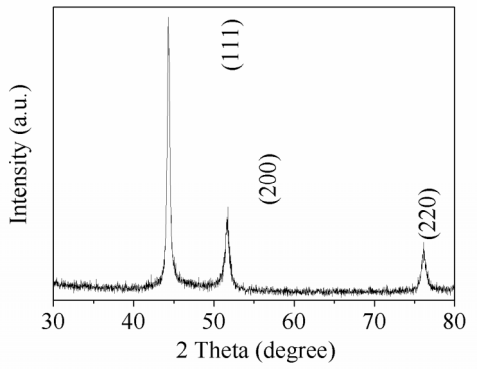

Figure 1. Typical XRD pattern of the product synthesized at 200˚C for 2 h.

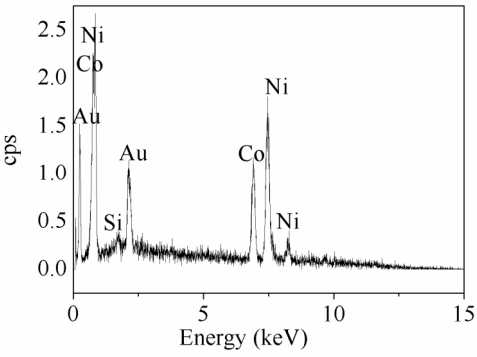

Figure 2. Typical EDS spectrum of the product synthesized at 200˚C for 2 h.

Copyright © 2011 SciRes.

conjunction with the XRD results in **Figure 1**, the success synthesis of high-purity fcc-phase CoNi product.

Figure 3(a) shows a low-magnification field emission scanning electron microscopy (FESEM) image of the CoNi product synthesized at 200˚C for 2 h. It is clear that the product is essentially chain-like CoNi assemblies with high uniformity of 20 μm - 30 μm in length. The chain-like assemblies can be classified as a type of hierarchical assemblies. **Figure 3(b)** displays the high-magnification FESEM image of the CoNi product. Each CoNi chain is assembled from CoNi submicrospheres with an average diameter of 800 nm. These submicrospheres serve as building block for the chains. Moreover, the surface of the CoNi submicrospheres is quite rough because they are composed of CoNi nanoparticles. **Figure 3(c)** illustrates the transmission electron microscopy (TEM) image of the CoNi product. It is seen that the product is chain-like CoNi assemblies of CoNi submicrospheres of average diameter 800 nm. The observation is consistent with those observed by FESEM in **Figures 3(a)-(b)**. In addition, bright contrast is not found inside the submicrospheres, indicating that they are solid rather than hollow submicrospheres. The inset of **Figure 3(c)** shows the electron diffraction pattern of a CoNi submicrosphere, revealing its polycrystalline nature. It is noted that the CoNi submicrospherical chains are very stable even subjected to an ultrasonic treatment of 30 min. This reflects that the chain-like CoNi assemblies are actually integrated and not simply aggregations of nanoparticles.

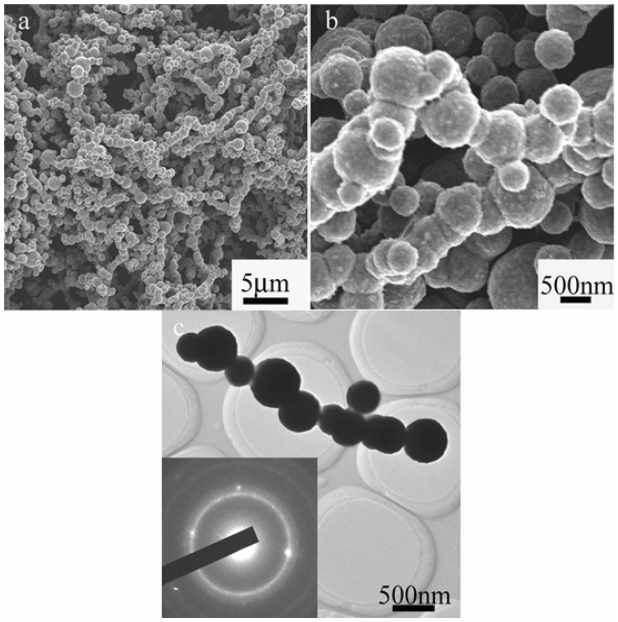

Figure 3. (a) Low-magnification FESEM image, (b) high-magnification FESEM image, and (c) TEM image of CoNi product synthesized at 200˚C for 2 h.

3.2. Effects of Surfactant and Reducing Agent on Morphology and Size

We found that the amounts of PVP surfactant and $N_2H_4{\cdot}H_2O$ reducing agent in the solution have the predominant effects on the morphology and size of the resulting CoNi products. In this section, we study the effects of PVP and $N_2H_4{\cdot}H_2O$ on the morphology and size of the CoNi products by keeping other reaction parameters unchanged.

Figure 4 shows scanning electron microscopy (SEM) images of CoNi products prepared using four different amounts of PVP at an optimal amount of $N_2H_4{\cdot}H_2O$ of 2 mL. In the absence of PVP, the CoNi submicrospherical chains self-assembled by CoNi submicrospheres as shown in **Figure 3** cannot be formed, but monodispersed microspheres with an average diameter of 1.5 μm are obtained instead (**Figure 4(a)**). When an increased amount of PVP of 0.3 g is used, the size of the microspheres is not uniform; it actually varies from 2 μm to 8 μm in diameter (**Figure 4(b)**). When the amount of PVP is increased to 0.7 g, chain-like assembles self-assembled from uniform submicrospheres of average diameter 800 nm are obtained (**Figure 4(c)**). When the amount of PVP is further increased to 1 g, chain-like assembles consisting of microspheres of average diameter 5 μm are formed (**Figure 4(d)**). The results suggest that the morphology and size of the CoNi products can be controlled by the amount of PVP. The optimal PVP is found to be 0.5 g, and the resulting CoNi submicrospherical chains are shown in **Figure 3**.

Figure 5 shows SEM images of CoNi products prepared using three different amounts of $N_2H_4{\cdot}H_2O$ at an

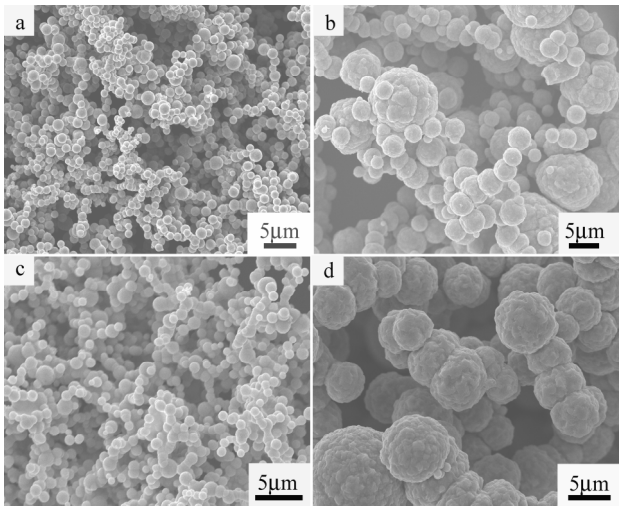

Figure 4. SEM images of CoNi products prepared using four different amounts of PVP of (a) 0 g, (b) 0.3 g, (c) 0.7 g, and (d) 1 g at an optimal amount of $N_2H_4{\cdot}H_2O$ of 2 mL.

Copyright © 2011 SciRes.

optimal amount of PVP of 0.5 g. With the addition of 0.5 mL of $N_2H_4{\cdot}H_2O$, the average diameter of microspheres is 10 μm (**Figure 5(a)**). When the amount of $N_2H_4{\cdot}H_2O$ is doubly increased to 1 mL, the average diameter of microspheres is half-reduced to 5 μm (**Figure 5(b)**). A further increase the amount of $N_2H_4{\cdot}H_2O$ to 2 mL leads to submicrospheres of average diameter 800 nm as reported in **Figure 3**. A subsequent increase the amount of $N_2H_4{\cdot}H_2O$ beyond 2 mL, e.g. 3 mL, cannot further decrease the size of the submicrospheres (**Figure 5(c)**). Therefore, the size of spheres in the CoNi products can be controlled by adjusting the amount of $N_2H_4{\cdot}H_2O$. In general, the size of spheres decreases with an increase in the amount of $N_2H_4{\cdot}H_2O$ up to 2 mL. The change in size of spheres is likely caused by the change in reaction rate. With increasing the amount of $N_2H_4{\cdot}H_2O$, the reaction rate is accelerated so that more nuclei are formed in the initial nucleation process and lead to the formation of more spheres with smaller diameters [19].

3.3. Possible Growth Mechanism

On the basis of the observed reaction phenomena and results, a possible growth mechanism for the formation of CoNi submicrospherical chains is addressed in this section. A similar mechanism for the growth of 1D magnetic cobalt chains has been presented in our early works [19,20]. As shown in **Figure 6**, three consecutive steps: namely: steps a, b, and c are possibly included in the growth mechanism. In step a, CoNi nanoparticles are reduced. This step actually includes three consequent processes. First, Co^{2+} and Ni^{2+} ions can combine with EG to form pink-mixed complexes $[Co(EG)_n]^{2+}$ and $[Ni(EG)_n]^{2+}$.

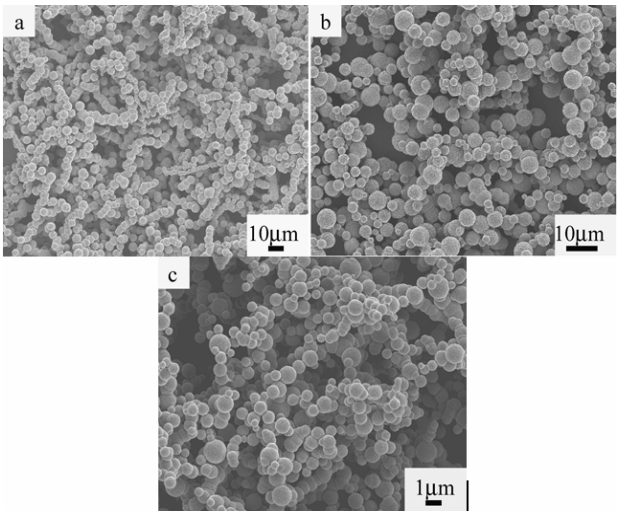

Figure 5. SEM images of CoNi products prepared using three different amounts of $N_2H_4{\cdot}H_2O$ of (a) 0.5 mL, (b) 1 mL, and (c) 3 mL at an optimal amount of PVP of 0.5 g.

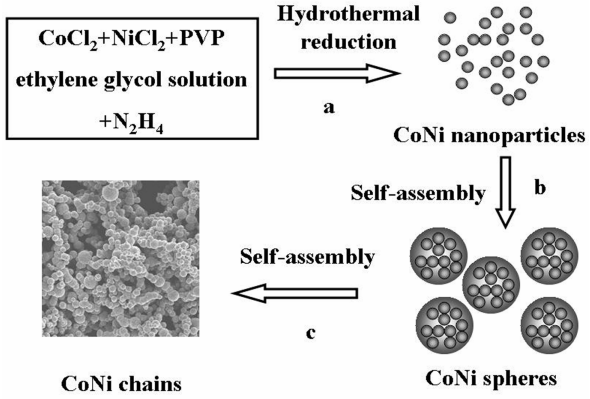

Figure 6. Schematic diagram of a possible growth mechanism for CoNi submicrospherical chains.

After $N_2H_4{\cdot}H_2O$ is added into the solution, the complexes react with $N_2H_4{\cdot}H_2O$ to give complexes of $[Co(N_2H_4)_3]^{2+}$ and $[Ni(N_2H_4)_3]^{2+}$ so that the solution turns turbid. The whole complex process can be expressed by the following two equations [21,22]:

$$\left[\mathrm{Co(EG)_n}\right]^{2+} + 3\mathrm{N_2H_4} \rightarrow \left[\mathrm{Co(N_2H_4)_3}\right]^{2+} + \mathrm{nEG} \quad (1)$$

$$\left[\mathrm{Ni(EG)_n}\right]^{2+} + 3\mathrm{N_2H_4} \rightarrow \left[\mathrm{Ni(N_2H_4)_3}\right]^{2+} + \mathrm{nEG} \quad (2)$$

Second, the complexes of $[Co(N_2H_4)_3]^{2+}$ and $[Ni(N_2H_4)_3]^{2+}$ can react with excessive hydrazine and thus reduce to Co and Ni nuclei at high temperature (at the boiling point of EG of 197˚C) even though they are stable at room temperature. The Co and Ni nuclei then form CoNi alloy nuclei. This reducing process accompanies the change in the color of the solution; that is, the solution is pink turbid and colorless before and after the reaction, respectively. The reducing process can be described by the following three equations:

$$\left[\mathrm{Co(N_2H_4)_3}\right]^{2+} + \mathrm{N_2H_4} \rightarrow \mathrm{Co}\downarrow + 4\mathrm{NH_3}\uparrow + \mathrm{N_2}\uparrow + \mathrm{H_2}\uparrow + 2\mathrm{H^+} \quad (3)$$

$$\left[\mathrm{Ni(N_2H_4)_3}\right]^{2+} + \mathrm{N_2H_4} \rightarrow \mathrm{Ni}\downarrow + 4\mathrm{NH_3}\uparrow + \mathrm{N_2}\uparrow + \mathrm{H_2}\uparrow + 2\mathrm{H^+} \quad (4)$$

$$\mathrm{Co} + \mathrm{Ni} \rightarrow \mathrm{CoNi} \quad (5)$$

In this reducing process, High reaction temperature is critical to simultaneously reduce the Co^{2+} and Ni^{2+} ions. If the reducing process is carried out at a lower temperature, for example, at 160˚C, elemental Co is found in the final product in addition to CoNi alloy. Third, the CoNi nuclei grow into CoNi nanoparticles. In step b, the CoNi nanoparticles diffuse and aggregate into CoNi spheres through an Ostwald ripening process [23] and the magnetic dipole-dipole interaction [24]. In step c, the CoNi

Copyright © 2011 SciRes.

spheres attach together and form chain-like assembles at magnetic dipole-dipole interaction and with the assistance of PVP.

3.4. Magnetic Properties

The magnetic hysteresis (*M-H*) loops of the CoNi submicrospherical chains synthesized at 200˚C for 2 h are shown in **Figure 7** for two different temperatures of 5 K and 295 K. The measurement was carried out with powder sample so that the CoNi submicrospherical chains were randomly oriented. It is clear that the *M-H* loops exhibit ferromagnetic characteristics with saturation magnetization (M_s) of 106.3 emu/g and 104.1 emu/g and coercivity (H_c) of 219 and 150 Oe at 5 K and 295 K, respectively. The M_s value of the CoNi submicrospherical chains at 295 K (room temperature) is almost the same as that of monodispersed CoNi submicrospheres of 105 emu/g, while the H_c value is higher than that of 34 Oe [25]. Compared with monodispersed CoNi submicrospheres, our CoNi submicrospherical chains have much larger length-to-diameter aspect ratios (*i.e.* 20 μm -30 μm : 800 nm). The increased aspect ratio gives rise to enhanced shape anisotropy, which may lead to an increased H_c. However, H_c of our CoNi submicrospherical chains is much lower than that of CoNi nanowires of 6000 Oe [26]. This may be ascribed to the smaller aspect ratios of our CoNi submicrospherical chains in comparison with the CoNi nanowires.

Figure 8 plots the temperature (*T*) dependence of zero field-cooled (ZFC) and field-cooled (FC) magnetizations (*M*) of the CoNi submicrospherical chains in the temperature range of 5 K - 295 K. For the ZFC process, the sample was first cooled from 295 K to 5 K without applied magnetic fields, and *M* was measured from 5 K to 295 K under an applied magnetic field of 50 Oe. For the FC process, *M* was measured while the sample was cooled from 295 K to 5 K,

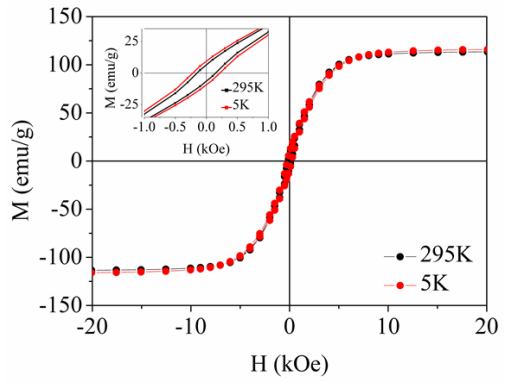

Figure 7. Magnetic hysteresis (*M-H*) loops of the CoNi submicrospherical chains synthesized at 200˚C for 2 h for two different temperatures of 5 K and 295 K.

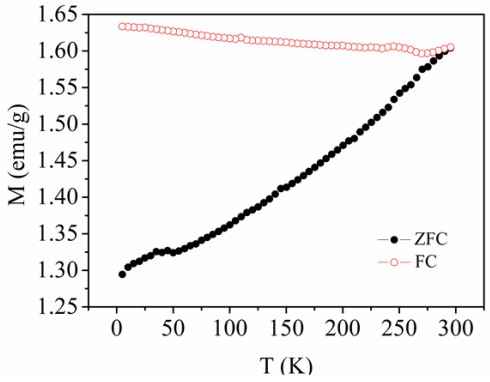

Figure 8. Temperature (*T*) dependence of zero field-cooled (ZFC) and field-cooled (FC) magnetizations (*M*) of the CoNi submicrospherical chains in the temperature range of 5 K -295 K.

i.e. in a cooling process. It is seen that the FC curve deviates from the ZFC curve, indicating an irreversible magnetic behavior. The increase in *M* with increasing *T* in the ZFC curve suggests a wide distribution of energy barrier in the CoNi submicrospherical chains which, in turn, may be due to the relatively wide distribution of particle size. No observable peak is found from the ZFC curve, indicating that the blocking temperature (T_B) is far above room temperature (295 K). The blocking temperature can be determined from the relation: $KV = 25k_BT_B$, where *K* is the effective anisotropy constant, *V* is the volume of particle, k_B=8.617×10^{-5} eV/K is the Boltzmann constant, and the product *KV* is the anisotropy energy barrier. Therefore, a high T_B implies a high *KV*, and the high *KV* mainly originates from the large shape anisotropy caused by aspect ratios in the CoNi submicrospherical chains.

4. Conclusions

We have synthesized highly anisotropic, highly pure magnetic CoNi submicrospherical chains by self-assembling fcc-phase CoNi submicrospheres via a surfactant- assisted solvothermal route under controlled amounts of PVP and $N_2H_4{\cdot}H_2O$ at 200˚C for 2 h without involving any nucleation agent. The influence of both surfactant and reducing agent on the morphology and size of the submicrospheres have been discussed, and a possible growth mechanism for the CoNi chains has been proposed. The CoNi chains have showed ferromagnetic characteristics with a low M_s of 104.1 emu/g and a high H_c of 150 Oe at 295 K compared to monodispersed CoNi submicrospheres as a result of their large shape anisotropy. It is expected that the CoNi chains have great prospect in a broad domain of industrial fields.

Copyright © 2011 SciRes.

5. References

[1] J. W. T. Heemskerk, Y. Noat, D. J. Bakker, J. M. Van Ruitenbeek, B. J. Thijsse and P. Klaver, "Current-Induced Transition in Atomic-Sized Contacts of Metallic Alloys," *Physical Review B*, Vol. 67, 2003, p. 115416. doi:10.1103/PhysRevB.67.115416

[2] S. H. Sun, "Recent Advances in Chemical Synthesis, Self-Assembly, and Applications of FePt Nanoparticles," *Advanced Materials*, Vol. 18, No. 4, 2006, pp. 393-403. doi:10.1002/adma.200501464

[3] J. Chen, D. H. Bradlurst, S. X. Dou and H. K. Liu, "Nickel Hydroxide as an Active Material for the Positive Electrode in Rechargeable Alkaline Batteries," *Journal of The Electrochemical Society*, Vol. 146, 1999, p. 3606. doi:10.1149/1.1392522

[4] D. Weller and M. E. Doerner, "Extremely High-Density Longitudinal Magnetic Recording Media," *Annual Review of Materials Science*, Vol. 30, 2000, pp. 611-644. doi:10.1146/annurev.matsci.30.1.611

[5] M. D. Lynch and D. L. Patrick, "Organizing Carbon Nanotubes with Liquid Crystals," *Nano Letters*, Vol. 2, No. 11, 2002, pp. 1197-1201. doi:10.1021/nl025694j

[6] K. M. Ryan, D. Erts, H. Olin, M. A. Morris and J. D. Holmes, "Three Dimensional Architectures of Ultra-High Density Semiconducting Nanowires Deposited on Chip," *Journal of the American Chemical Society*, Vol. 125, No. 20, 2003, pp. 6284-6288. doi:10.1021/ja0345064

[7] S. D. Hersee, X. Y. Sun and X. Wang, "The Controlled Growth of GaN Nanowires," *Nano Letters*, Vol. 6, No. 8, 2006, pp. 1808-1811. doi:10.1021/nl060553t

[8] H. C. Zeng, J. Lin, W. K. Teo, J. C. Wu and K. L. Tan, "Monoclinic ZrO_2 and Its Supported Materials Co/Ni/ZrO_2 for N_2O Decomposition," *Journal of Materials Research*, Vol. 10, 1995, p. 545. doi:10.1557/JMR.1995.0545

[9] C. Sangregorio and C. D. Fernandez, "Superparamagnetism and Coercivity in HCP-Co Nanoparticles Dispersed in Silica Matrix," *Journal of Magnetism and Magnetic Materials*, Vol. 272, 2004, p. e1251. doi:10.1016/j.jmmm.2004.01.062

[10] E. Gomez, S. Pane and E. Valles, "Electrodeposition of Co-Ni and Co-Ni-Cu Systems in Sulphate-Citrate Medium," *Electrochimica Acta*, Vol. 51, 2005, p. 146. doi:10.1016/j.electacta.2005.04.010

[11] K. V. P. M. Shafi, A. Gedanken and R. Prozorov, "Sonochemical Preparation and Characterization of Nanosized Amorphous Co-Ni Alloy Powders," *Journal of Materials Chemistry*, Vol. 8, 1998, pp. 769-773. doi:10.1039/a706871i

[12] T. Syukri, Y. Ban, Y. Ohya, Takahashi, "A Simple Synthesis of Metallic Ni and Ni–Co Alloy Fine Powders from a Mixed-Metal Acetate Precursor," *Materials Chemistry and Physics*, Vol. 78, 2003, p. 645. doi:10.1016/S0254-0584(02)00185-2

[13] G. Viau, F. Fievet-Vincent and F. Fievet, "Nucleation and Growth of Bimetallic CoNi and FeNi Monodispersed Particles Prepared in Polyols," *Solid State Ionics*, Vol. 84, No. 3-4, 1996, pp. 259-270. doi:10.1016/0167-2738(96)00005-7

[14] P. Toneguzzo, G. Viau, O. Acher, F. Guillet, E. Bruneton and F. Fievet-Vincent, "CoNi and FeCoNi Fine Particles Prepared by the Polyol Process: Physico-Chemical Characterization and Dynamic Magnetic Properties," *Journal of Materials Science*, Vol. 35, No. 15, 2000, pp. 3767-3784. doi:10.1023/A:1004864927169

[15] Y. D. Li, L. Q. Li, H. W. Liao and H. R. Wang, "Preparation of Pure Nickel, Cobalt, Nickel-Cobalt and Nickel-Copper Alloys by Hydrothermal Reduction," *Journal of Materials Chemistry*, Vol. 9, 1999, pp. 2675-2677. doi:10.1039/a904686k

[16] D. Ung, G. Viau, C. Ricolleau, F. Warmont, P. Gredin and F. Fiver, "CoNi Nanowires Synthesized by Heterogeneous Nucleation in Liquid Polyol," *Advanced Materials*, Vol. 17, No. 3, 2005, pp. 338-344. doi:10.1002/adma.200400915

[17] L. P. Zhu, H. M. Xiao and S. Y. Fu, "Surfactant-Assisted Synthesis and Characterization of Novel Chain-Like CoNi Alloy Assemblies," *European Journal of Inorganic Chemistry*, Vol. 2007, No. 25, 2007, pp. 3947-3951. doi:10.1002/ejic.200700558

[18] M. J. Hu, Y. Lu, S. Zhang, S. R. Guo, B. Lin, M. Zhang and S. H. Yu, "High Yield Synthesis of Bracelet-Like Hydrophilic Ni-Co Magnetic Alloy Flux-Closure Nanorings," *Journal of the American Chemical Society*, Vol. 130, No. 35, 2008, pp. 11606-11607. doi:10.1021/ja804467g

[19] Y. J. Zhang, Q. Yao, Y. Zhang, T. Y. Cui, D. Li, W. Liu, W. Lawrence and Z. D. Zhang, "Solvothermal Synthesis of Magnetic Chains Self-Assembled by Flowerlike Cobalt Submicrospheres," *Crystal Growth & Design*, Vol. 8, No. 9, 2008, pp. 3206-3212. doi:10.1021/cg7010452

[20] Y. J. Zhang, S. Ma, D. Li, Z. H. Wang and Z. D. Zhang, "Surfactant-Assisted Hydrothermal Synthesis of Chains Self-Assembled by Cobalt Microspheres," *Materials Research Bulletin*, Vol. 43, No. 8-9, 2008, pp. 1957-1965. doi:10.1016/j.materresbull.2007.11.010

[21] Y. C. Zhu, H. G. Zheng, Q. Yang, A. L. Pan, Z. P. Yang and Y. T. Qian, "Growth of Dendritic Cobalt Nanocrystals at Room Temperature," *Journal of Crystal Growth*, Vol. 260, No. 3-4, 2004, pp. 427-434. doi:10.1016/j.jcrysgro.2003.08.037

[22] C. M. Liu, L. Guo, R. M. Wang, Y. Deng, H. B. Xu and S. H. Yang, "Magnetic Nanochains of Metal Formed by Assembly of Small Nanoparticles," *Chemical Communications*, Vol. 23, 2004, pp. 2726-2727. doi:10.1039/b411311j

[23] A. R. Roosen and W. C. Carter, "Simulations of Microstructural Evolution: Anisotropic Growth and Coarsening," *Physica A*, Vol. 261, No. 1-2, 1998, pp. 232-247. doi:10.1016/S0378-4371(98)00377-X

[24] V. Salgueirino-Maceira, M. A. Correa-Duarte, A. Hucht and M. Farle, "One-Dimensional Assemblies of Silica-Coated Cobalt Nanoparticles: Magnetic Pearl Necklaces," *Journal of Magnetism and Magnetic Materi-*

Copyright © 2011 SciRes.

als, Vol. 303, No. 1, 2006, pp. 163-166. doi:10.1016/j.jmmm.2005.11.003

[25] P. Elumalai, H. N. Vasan, M. Verelst, P. Lecante, V. Carles and P. Taihades, "Synthesis and Characterization of Sub-Micron Size Co-Ni Alloys using Malonate as Precursor," *Materials Research Bulletin*, Vol. 37, No. 2, 2002, pp. 353-363. doi:10.1016/S0025-5408(01)00768-1

[26] D. Ung, Y. Soumare, N. Chakroune, G. Viau, M. J. Vaulay, V. Richard and F. Fiévet, "Growth of Magnetic Nanowires and Nanodumbbells in Liquid Polyol," *Chemistry of Materials*, Vol. 19, No. 8, 2007, pp. 2084-2094. doi:10.1021/cm0627387

[27] Z. D. Zhang, J. G. Zheng, I. Skorvanek, G. H. Wen, J. Kovac, F. W. Wang, J. L. Yu, J. J. Li, X. L. Dong, S. R. Jin, W. Liu, and X. X. Zhang, "Shell/Core Structure and Magnetic Properties of Carbon-Coated Fe-Co(C) Nanocapsules," *Journal of Physics*: *Condensed Matter*, Vol. 13, No. 9, 2001, p. 1921. doi:10.1088/0953-8984/13/9/314

Copyright © 2011 SciRes.